M&C 2001 Salt Lake City, Utah, USA, September 2001.

MULTIGROUP TRANSIENT CALCULATION WITHIN THE FRAMEWORK OF A TWO-GROUP HEXAGONAL CMFD FORMULATION

Han Gyu Joo, Jin Young Cho, Jae Seung Song, and Sung Quun Zee
Korea Atomic Energy Research Institute
P.O. Box 105, Yusong, Taejon, 305-600, Korea
joohan; jyoung; jssong; zee@kaeri.re.kr

Thomas J. Downar
Purdue University
1290 Nuclear Engineering Bldg., W. Lafayette, IN 47907-1290, U. S. A.
downar@ecn.purdue.edu

Keywords: Multigroup, Dynamic Condensation, CMFD, One-Node Kernel

ABSTRACT

A two-group CMFD formulation capable of solving multigroup problems in hexagonal geometry is established by incorporating a dynamic condensation scheme. A multigroup one-node kernel employing a two-dimensional polynomial expansion within a triangle is derived such that it provides a nodal spectrum as well as multigroup interface currents. The accuracy and computational efficiency of the two-group CMFD based multigroup calculation method are demonstrated by solving multigroup eigenvalue benchmark problems. The improvement effects attainable by multigroup calculations are then investigated by analyzing a model core with four different group structures. The eigenvalue calculation results show that the current two-group solution approach involves only trivial errors. However, it is also shown from control rod ejection calculations that the error in the transient core power behavior can be significant due to small errors in the ejected rod worth as well as the inability of distinguishing the delayed and prompt neutron spectra in two-group calculations.

1. INTRODUCTION

The two-group formulation has been successfully used in thermal reactor calculations. A long history of good agreement between predictions and measurements obtained in operating light water reactors (LWRs) supports the success. Because of the adequacy of the two-group formulation, most nodal diffusion codes used for design analyses of LWRs have only a hard-wired two-group calculation feature. These codes therefore cannot be used for multigroup calculations, which are required in the circumstances that the reactor involves hardened spectra, strong leakages or severe heterogeneity. Besides the fast reactors and small research reactors, such circumstances can be encountered in some thermal reactors with advanced fuel designs involving MOX

or thorium. Implementation of a multigroup feature into an existing two-group code is thus often desired to extend the code's applicability. This paper first deals with a multigroup calculation method that can be readily implemented into a two-group code by retaining the basic two-group calculation structure, and then investigates the significance of multigroup calculations in transient analyses.

Suppose that a converged multigroup solution is available. Then it is possible to reduce the multigroup problem into an equivalent two-group problem by condensing the nodal multigroup constants. As long as the interface currents as well as nodal reaction rates are conserved during the condensation, a consistent two-group model can be obtained. Consistent condensation can be performed with a partially converged multigroup solution as well during an iterative solution process. The resulting two-group problem and its solution can be used to accelerate the convergence of the overall iteration. In the point of view of the two-group calculation, the trial multigroup solution provides nodal *spectra* to be used in the condensation. In the work here, the concept of *dynamic condensation* involving iterative updates of nodal spectra is introduced in order to perform multigroup calculations within the framework of a two-group formulation.

The coarse mesh finite difference (CMFD) formulation (Sutton, 1996) is well suited for the realization of dynamic condensation in that the global CMFD problem can remain in the two-group structure while the local higher-order problem (either a two-node or one-node problem) is constructed with a multigroup structure. The nodal coupling relations representing the interface current with the two node average fluxes can be setup in the two-group structure by conserving the condensed multigroup currents determined by the local problem solutions, which specify the spectra as well to be used for generating nodal two-group constants. In the work here, a two-group hexagonal CMFD formulation employing a two-group one-node kernel (Cho, 2001) is extended for a multigroup capability. In this approach, most of the two-group CMFD calculation methods can remain intact and only a multigroup one-node kernel needs to be added.

Since nodal spectra as well as nodal coupling relations should be the primary outputs of the one-node kernel, the multigroup one-node kernel must be constructed such that it can determine the node-average multigroup fluxes uniquely. In the following section, a multigroup one-node kernel that solves a three-dimensional problem defined for a hex-octahedron domain is derived. In order to implement the multigroup one-node kernel into the two-group CMFD formulation, a special nonlinear iteration scheme has to be established since a prolongation operation is required to provide multigroup boundary conditions from a two-group CMFD solution. The nonlinear iteration scheme coordinating the multigroup one-node calculations and the two-group CMFD calculations is presented in Section 3. The performance of the present multigroup calculation method is examined in Section 4 by solving known multigroup benchmark problems and evaluating the accuracy and computing times. In order to examine the improvements attainable by multigroup calculations, multigroup reactor calculations are performed with various group structures. The accuracy of the multigroup and two-group solutions for eigenvalue and transient problems is investigated in Section 5.

2. MULTIGROUP ONE-NODE TPEN KERNEL

The TPEN (Triangle-based Polynomial Expansion Nodal) method (Cho, 2001) solves two transverse-integrated neutron diffusion equations for a hex-octahedron node. One is the radial equation defined for a hexagon and the other is the axial equation defined for the z-direction. The radial problem is solved by splitting the hexagon into six triangles and then by employing a polynomial expansion of flux within each triangle. Given the incoming current boundary conditions, the solutions of the two separate transverse-integrated equations yield two sets of node average group fluxes rather than one. This is not a problem in the two-group problem since only the outgoing currents need to be taken from the one-node solution. In the multigroup problem, however, a unique set of group fluxes is desired because the node average group fluxes determine the nodal spectra to be used in the group constant generation for the two-group CMFD problem. In this regard, a simultaneous solution of the two transverse equations is derived in this section. For an efficient solution of general multigroup problems, the fission source terms are moved to the right hand side to avoid the direct inversion of the group block. The following subsection first presents the balance equations and then the subsequent subsections describe the coupled TPEN solution procedure.

2.1 Coupled Transverse-Integrated Neutron Diffusion Equations

The transverse-integrated neutron diffusion equations defined for the hex-octahedron domain shown in Fig. 1 consist of six radial and one axial equations. With index *m* denoting the *m*-th triangle, the balance equations can be written as:

$$-D_g\left(\frac{\partial^2}{\partial x^2}+\frac{\partial^2}{\partial y^2}\right)\phi_g^{Rm}(x,y)+\Sigma_{rg}\phi_g^{Rm}(x,y)-\sum_{g'<g}\Sigma_{g'g}\phi_{g'}^{Rm}(x,y) = Q_g^{Rm}(x,y)-L_g^{Zm}(x,y), \quad m=1..6 \tag{1}$$

$$-D_g\frac{\partial^2}{\partial z^2}\phi_g^{Z}(z)+\Sigma_{rg}\phi_g^{Z}(z)-\sum_{g'<g}\Sigma_{g'g}\phi_{g'}^{Z}(z)=Q_g^{Z}(z)-L_g^{R}(z) \tag{2}$$

where

$$Q_g^{U}(u)=\frac{\chi_g}{k_{eff}}\sum_{g'}\nu\Sigma_{fg'}\phi_{g'}^{R,old}(u)+\sum_{g'>g}\Sigma_{g'g}\phi_{g'}^{R,old}(u)+S_g^{TFS}(u)\ , \quad u=(x,y)\text{ or }z\,, \tag{3}$$

$$L_g^{Zm}(x,y)=\frac{1}{h_Z}\left(J_{gT}^{Zm}(x,y)-J_{gB}^{Zm}(x,y)\right),\text{ and} \tag{4}$$

$$L_g^{R}(z)=\frac{2\sqrt{3}}{9h_R}\sum_{u=1}^{3}\left(J_{g(u+3)}^{x}(z)-J_{gu}^{x}(z)\right)\,. \tag{5}$$

Here the source term Q contains the fission and upscattering sources, and in addition, the transient fixed source (TFS) appearing in the transient formulation. The source distribution is assumed to be known from the previous iterate of the flux distribution. The transverse-leakage sources represented by Eqs. (4) and (5) have spatial dependence which is to be determined, in the TPEN approach, by the node average transverse leakages of the neighboring nodes as well as the node of interest itself. In the original TPEN formulation, all the transverse leakages are considered known and thus the two balance equations are independent and can be solved separately. In this derivation, however, the transverse-leakage of the node of interest is treated unknown so that the radial and axial equations are now coupled through the transverse leakages.

2.2 TPEN Solution Procedure

The radial equation above, Eq. (1), is solved by representing the intranodal flux within the triangle by a nine-term, two-dimensional polynomial of the following form:

$$\phi_g^{Rm}(x,y) = c_{g0}^m + a_{gx}^m x + a_{gy}^m y + b_{gx}^m x^2 + b_{gu}^m u^2 + b_{gp}^m p^2 + c_{gx}^m x^3 + c_{gu}^m u^3 + c_{gp}^m p^3 \quad (6)$$

where

$$u = -\frac{1}{2}x - \frac{\sqrt{3}}{2}y \text{ and } p = -\frac{1}{2}x + \frac{\sqrt{3}}{2}y. \quad (7)$$

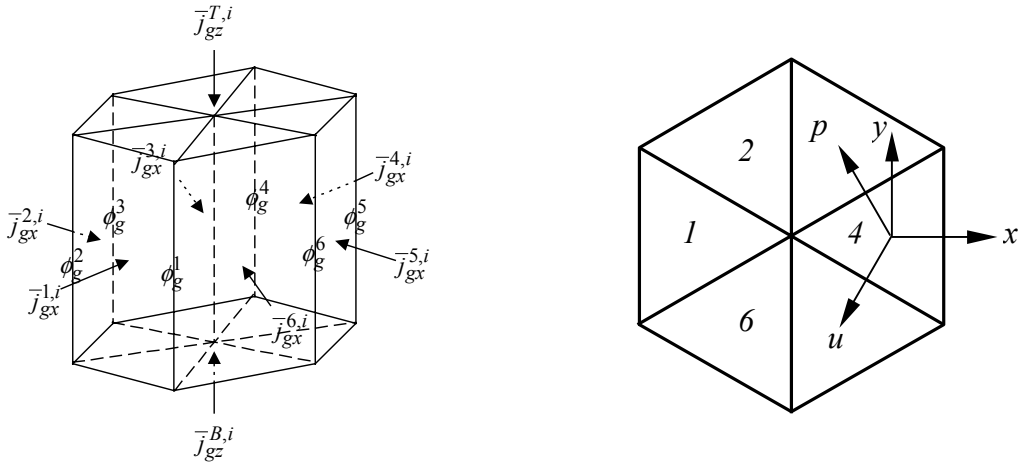

* *A local coordinate is set for each triangle and the outward normal direction at each hexagon surface is taken as the positive x-direction of the local coordinate.*

Fig. 1 Geometry, Boundary Conditions and Coordinates for TPEN

The nine coefficients of the third-order polynomial are related with the following nine unknowns: 3 surface average fluxes, 3 corner point fluxes, node average flux, first order *x*-and *y*-moments of the flux. To determine the nine unknowns, nine constraint conditions

are imposed: 3 surface average current continuity conditions, 3 corner point leakage balance (CPB) conditions, nodal balance condition, first-order *x*-moment balance condition, and first order *y*-moment balance condition. On the other hand, the axial equation is solved by the nodal expansion method (NEM) that involves five unknowns: first- and second-order *z*-moments as well as the two surface average fluxes and node average flux.

Because the TPEN method requires two directional first-order moments, the corresponding moments of the source terms appearing in Eq. (1) need to be specified. These moments carry the spatial dependence of the source. In the TPEN, the source shape is approximated by a seven-term, two-dimensional polynomial and the seven coefficients are determined by preserving the node average values of the source at the six surrounding nodes and the node of interest. For the one hexagon node problem, there are six sets of unknowns, one for each triangle. In order to determine uniquely all the coefficients of the six sets, six hexagon-corner point fluxes as well as six surface average incoming currents need to be specified per group. The hexagon-corner point fluxes are determined before solving the one-node problems by imposing the CPB condition to each hexagon-corner. In order to obtain the corner point leakage, the intranodal flux distribution within the *hexagon* is approximated by a thirteen-term polynomial whose coefficients are expressed with 6 surface average fluxes, 6 corner point fluxes, and the node average flux of the hexagon (Cho, 1999). During the CPB calculation, the node average and surface average fluxes are assumed to be known, and only the corner point fluxes are taken as the unknowns so that the CPB conditions yield a linear system for corner point fluxes at each plane. The linear system is solved by the plain Gauss-Seidel method. More detailed explanations of the TPEN solution procedure outlined above are provided in the original TPEN paper (Cho, 2001) with relevant equations.

2.3 Direct Transverse-Leakage Coupling

Among various constraint conditions, only the nodal balance and moment equations contain terms originating from the RHS terms of Eqs. (1) and (2). Hence the node average and directional moments of the sources including the transverse-leakages should be obtained. For the solution of the radial equation, the axial leakage's node average value (0-th order moment) and the *x*- and *y*-directional first order moments are required. Each of these moments (including the 0-th order moment for the node average) consists of two components: one from the contribution of axial leakage of the hexagon of interest node and the other from the six neighboring hexagons. Namely,

$$\bar{L}_g^{Zm} = \bar{L}_{g,neig}^{Zm} + \frac{1}{h_Z} \sum_{s=T,B} \left(\bar{J}_{gs}^{Zo} - \bar{J}_{gs}^{Zi} \right) \quad \text{and} \tag{8}$$

$$\tilde{L}_{gu}^{Zm} = \tilde{L}_{gu,neig}^{Zm} + \frac{\mu_{gu}^{Rm}}{h_Z} \sum_{s=T,B} \left(\bar{J}_{gs}^{Zo} - \bar{J}_{gs}^{Zi} \right), \quad u=x,y \tag{9}$$

where the partial currents replace the net current appearing in Eq. (4). Note that $\mu_{gy,neig}^{Zm} = 0$. The contribution from the neighboring hexagons induces a gradient of the axial leakage within the hexagon, and thus the contribution from the neighbors must be different for each triangle so that the first term above retains the triangle index *m*. The contribution of the hexagon of interest, however, is constant over the hexagon and thus no dependence on the triangle location appears in the second term. Since the incoming currents are given as the boundary conditions, the actual unknown in the axial leakage moment given by Eqs. (8) and (9) is the surface average outgoing partial current at the top and bottom of the hex-octahedron node. These unknown terms should be moved to the left hand side of the nodal balance and the moment equations.

The moments of the radial leakage can be similarly represented for the axial equation. Since moments are required up to the second-order in the NEM used for the axial solution, three moments are defined as follows:

$$\bar{L}_g^R = \frac{2\sqrt{3}}{9h_R}\sum_{m=1}^{6}\left(\bar{J}_{gm}^{xo} - \bar{J}_{gm}^{xi}\right) \text{ and} \tag{10}$$

$$\tilde{L}_{gq}^R = \tilde{L}_{gq,neig}^R + \mu_q^Z \bar{L}_g^R \ , \ q=1,2. \tag{11}$$

With the representations of the radial leakage moments given by Eqs. (10) and (11), the hexagon surface outgoing partial currents appear in the axial nodal balance equation, 1-st and 2-nd order axial moment equations. These radial partial current terms should be moved to the left hand side because they are unknowns as well.

2.4 One-Node Linear System and Its Solution

For the hex-octahedron shown in Fig. 1, 36 unknowns are defined per group for the coupled TPEN. They are 6 hexagon surface outgoing partial currents, 6 inner surface average fluxes, 6 triangle average fluxes, 6 *x*-moments, 6 *y*-moments, 1 center point flux, 2 axial partial currents (top and bottom), 1 first-order *z*-moment, and 1 second-order *z*-moment, and finally 1 hexagon average flux. The constraint conditions required to determine these unknowns are as follows: 6 triangle nodal balance conditions, 6 triangle *x*-moment equations, 6 triangle *y*-moment equations, 6 inner surface current continuity conditions, 6 radial incoming current boundary conditions, 1 center point CPB condition, 2 axial incoming current boundary conditions, 1 first-order *z*-moment equation, 1 second-order *z*-moment equation, and 1 hexagon average flux constraint which states the average of the 6 triangle average fluxes is the same as the hexagon average flux. The linear system consisting of these constraints and unknowns can be represented by Eq. (12) for a given group where **A, X, Y, S** and $\mathbf{C^R}$ are 6x6 matrices while $\mathbf{C^Z}$ is a 2x2 matrix. Other matrices are all 1x1. The dimensions of the unknown vectors are defined accordingly.

The 36x36 linear system can be reduced algebraically to one equation. The order of elimination of the unknowns to reduce the linear system is as follows: $\bar{\boldsymbol{\varphi}}_{\mathbf{H}}$, $\bar{\boldsymbol{\varphi}}$, $\tilde{\boldsymbol{\varphi}}_{\mathbf{x}}$, $\tilde{\boldsymbol{\varphi}}_{\mathbf{y}}$,

$\bar{\mathbf{J}}_{\mathbf{o}}^{\mathbf{R}}$, $\bar{\boldsymbol{\varphi}}_{\mathbf{s}}$, $\bar{\boldsymbol{\varphi}}_{\mathbf{p}}$, $\bar{\mathbf{J}}_{\mathbf{o}}^{\mathbf{Z}}$, $\tilde{\boldsymbol{\varphi}}_{\mathbf{z}}^{\mathbf{S}}$, and $\tilde{\boldsymbol{\varphi}}_{\mathbf{z}}^{\mathbf{F}}$. With this sequence of elimination, the first unknown to be determined is the first-order *z*-moment and the back substitution performed in the reverse order determines finally the hexagon average flux.

$$\begin{bmatrix}
\mathbf{A}_1 & \mathbf{0} & \mathbf{0} & \mathbf{A}_2 & \mathbf{A}_3 & \mathbf{A}_4 & \mathbf{A}_5 & \mathbf{0} & \mathbf{0} & \mathbf{0} \\
\mathbf{0} & \mathbf{X}_1 & \mathbf{0} & \mathbf{X}_1 & \mathbf{X}_2 & \mathbf{X}_3 & \mathbf{X}_4 & \mathbf{0} & \mathbf{0} & \mathbf{0} \\
\mathbf{0} & \mathbf{0} & \mathbf{Y}_1 & \mathbf{Y}_2 & \mathbf{0} & \mathbf{0} & \mathbf{0} & \mathbf{0} & \mathbf{0} & \mathbf{0} \\
\mathbf{S}_1 & \mathbf{S}_2 & \mathbf{S}_3 & \mathbf{S}_4 & \mathbf{0} & \mathbf{S}_5 & \mathbf{0} & \mathbf{0} & \mathbf{0} & \mathbf{0} \\
\mathbf{C}_1^{\mathbf{R}} & \mathbf{C}_2^{\mathbf{R}} & \mathbf{0} & \mathbf{0} & \mathbf{C}_3^{\mathbf{R}} & \mathbf{C}_4^{\mathbf{R}} & \mathbf{0} & \mathbf{0} & \mathbf{0} & \mathbf{0} \\
\mathbf{0} & \mathbf{P}_1 & \mathbf{0} & \mathbf{0} & \mathbf{P}_2 & \mathbf{P}_3 & \mathbf{0} & \mathbf{0} & \mathbf{0} & \mathbf{0} \\
\mathbf{0} & \mathbf{0} & \mathbf{0} & \mathbf{0} & \mathbf{0} & \mathbf{0} & \mathbf{C}_2^{\mathbf{Z}} & \mathbf{C}_3^{\mathbf{Z}} & \mathbf{C}_4^{\mathbf{Z}} & \mathbf{C}_5^{\mathbf{Z}} \\
\mathbf{0} & \mathbf{0} & \mathbf{0} & \mathbf{0} & \mathbf{Z}_1^{\mathbf{F}} & \mathbf{0} & \mathbf{Z}_2^{\mathbf{F}} & \mathbf{Z}_3^{\mathbf{F}} & \mathbf{0} & \mathbf{0} \\
\mathbf{0} & \mathbf{0} & \mathbf{0} & \mathbf{0} & \mathbf{Z}_2^{\mathbf{S}} & \mathbf{0} & \mathbf{Z}_3^{\mathbf{S}} & \mathbf{0} & \mathbf{Z}_4^{\mathbf{S}} & \mathbf{Z}_5^{\mathbf{S}} \\
\mathbf{I}_6 & \mathbf{0} & \mathbf{0} & \mathbf{0} & \mathbf{0} & \mathbf{0} & \mathbf{0} & \mathbf{0} & \mathbf{0} & -\mathbf{6}
\end{bmatrix}
\begin{bmatrix}
\bar{\boldsymbol{\varphi}} \\ \tilde{\boldsymbol{\varphi}}_{\mathbf{x}} \\ \tilde{\boldsymbol{\varphi}}_{\mathbf{y}} \\ \bar{\boldsymbol{\varphi}}_{\mathbf{s}} \\ \bar{\mathbf{J}}_{\mathbf{o}}^{\mathbf{R}} \\ \boldsymbol{\varphi}_{\mathbf{p}} \\ \bar{\mathbf{J}}_{\mathbf{o}}^{\mathbf{Z}} \\ \tilde{\boldsymbol{\varphi}}_{\mathbf{z}}^{\mathbf{F}} \\ \tilde{\boldsymbol{\varphi}}_{\mathbf{z}}^{\mathbf{S}} \\ \bar{\boldsymbol{\varphi}}_{\mathbf{H}}
\end{bmatrix} =
\begin{bmatrix}
\bar{\mathbf{S}} \\ \tilde{\mathbf{S}}_{\mathbf{x}} \\ \tilde{\mathbf{S}}_{\mathbf{y}} \\ \bar{\mathbf{S}}_{\mathbf{s}} \\ \bar{\mathbf{S}}_{\mathbf{o}}^{\mathbf{R}} \\ \mathbf{S}_{\mathbf{p}} \\ \bar{\mathbf{S}}_{\mathbf{o}}^{\mathbf{Z}} \\ \tilde{\mathbf{S}}_{\mathbf{z}}^{\mathbf{F}} \\ \tilde{\mathbf{S}}_{\mathbf{z}}^{\mathbf{S}} \\ \mathbf{0}
\end{bmatrix} . \qquad (12)$$

3. COORDINATION OF MULTIGROUP KERNEL AND TWO-GROUP CMFD

The solution of the multigroup one-node problem provides multigroup node-average fluxes as well as multigroup interface currents. The multigroup fluxes define the nodal spectrum to be used in the dynamic condensation of the multigroup cross sections which is performed by spectrum weighting as follows:

$$\hat{\Sigma}_{\alpha G} = \sum_{g \in G} \varphi_g \Sigma_{\alpha g} , \quad G=1 \text{ or } 2 \qquad (13)$$

where

$$\varphi_g = \frac{\phi_g}{\hat{\phi}_G} \quad \text{and} \quad \hat{\phi}_G = \sum_{g \in G} \phi_g . \qquad (14)$$

On the other hand, the multigroup interface current is used to determine the two-group corrective nodal coupling coefficient by the following equation:

$$\hat{D}_G = -\frac{\tilde{D}_G \left(\hat{\phi}_G^l - \hat{\phi}_G^r \right) + \hat{J}_G}{\hat{\phi}_G^l + \hat{\phi}_G^r} \qquad (15)$$

where $\tilde{D}_G$ is the finite difference based nodal coupling coefficient and

$$\hat{J}_G = \sum_{g \in G} J_g \ . \qquad (16)$$

Once the corrective nodal coupling is determined, the two-group interface current can be represented as a linear combination of the two-group node average fluxes of the left and right nodes of the interface as follows:

$$J_G^{CMFD} = -\tilde{D}_G\left(\phi_G^{r,CMFD} - \phi_G^{l,CMFD}\right) - \hat{D}_G\left(\phi_G^{r,CMFD} + \phi_G^{l,CMFD}\right). \tag{17}$$

With this nodal coupling relation and the two-group constants, the CMFD linear system then can be formulated. The solution of the CMFD linear system yields a two-group flux distribution. At convergence of the nonlinear iteration, the two-group nodal reaction rates preserve the corresponding multigroup reaction rates.

Once a two-group CMFD solution is obtained, the boundary conditions for the multigroup one-node problems have to be established by prolongation of the two-group information into the multigroup one. The prolongation can be achieved simply by using the multigroup shapes obtained in the previous one-node calculation. The multigroup shape for the flux would just be the spectrum used for group constant condensation. Additionally, the multigroup shape for the outgoing partial current is required to specify the multigroup incoming current conditions as well as the transverse leakages. The multigroup outgoing currents are obtained as follows by using the outgoing current spectra:

$$J_g^{o,n+1} = \varsigma_g^n \hat{J}_G^{o,n+1} \tag{18}$$

where

$$\varsigma_g^n = \frac{J_g^{o,n}}{\hat{J}_G^{o,n}} \quad \text{and} \quad \hat{J}_G^{o,n} = \sum_{g \in G} J_g^{o,n}. \tag{19}$$

The multigroup flux of the hexagonal node is obtained similarly using the spectra and then used to update the multigroup moments of the triangular nodes.

The multigroup one-node TPEN kernel incorporating the derivation given in the previous section has been implemented into the PARCS code (Joo, 1998), which already had a two-group hexagonal CMFD solver. During the implementation, the nonlinear iteration scheme shown in Fig. 2 was incorporated in order to control the alternate calculations of the two-group CMFD and multigroup one-node TPEN calculations. As indicated in the figure, the T-H feedback on cross sections is performed in the multigroup structure and the multigroup cross sections are condensed into two groups using the nodal spectra determined by the multigroup TPEN kernel. The β_s factor shown in the figure is the surface flux correction factor and is used in the similar manner as D-hat to obtain the surface flux from the node average fluxes. The two-group surface flux and the net current determine the two-group partial current to be used in the multigroup prolongation of the outgoing partial current for TPEN. In the TPEN calculation, several sweeps (N_s) of the one-node problem is performed to achieve sufficient convergence of the multigroup solution.

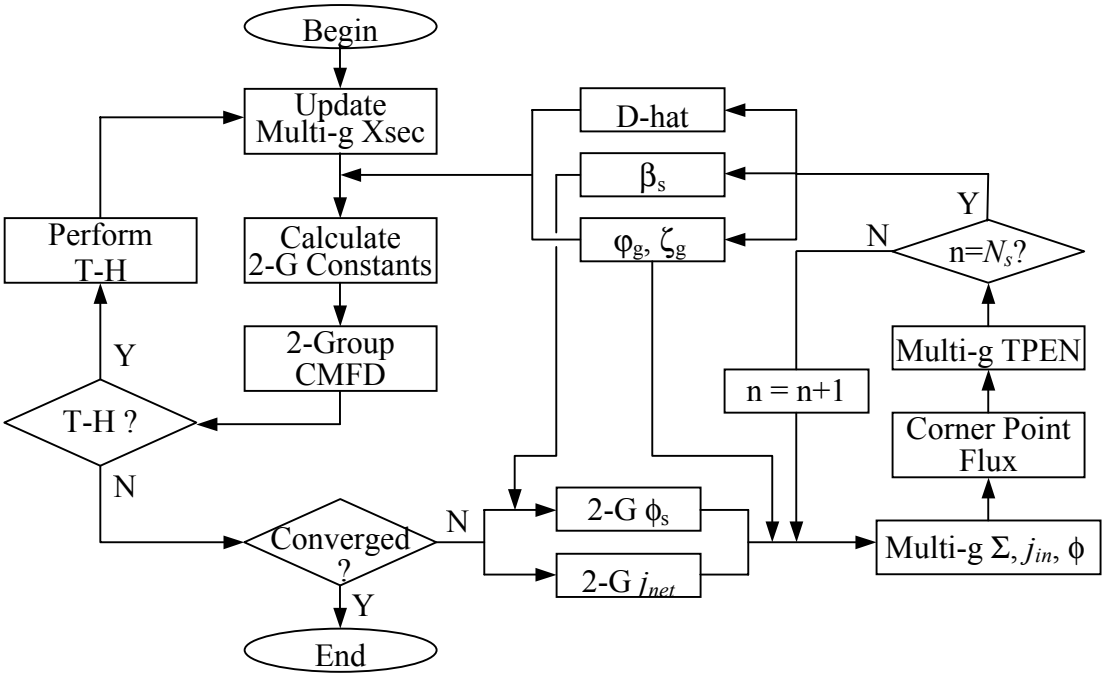

Fig. 2 Nonlinear Iteration Scheme for Controlling 2-G CMFD and Multigroup TPEN

4. EIGENVALUE BENCHMARK CALCULATIONS

In order to examine the performance of the presented multigroup calculation method, two hexagonal multigroup eigenvalue problems have been analyzed and the solution accuracy and the convergence characteristics were evaluated. The first problem is the SNR 4 group problem (ANL, 1985), which has been solved by many other codes. The core consists of 289 assemblies loaded into a hexagonal array with a pitch of 20 cm. The PARCS model for this core was made with 30° symmetry, 8 planes, and the first coarse group (in the two group structure) representing Groups 1 and 2 of the 4 groups. The second problem is the BFS75 9-group problem (Kim, 1999), which represents a fast reactor critical experiment core consisting of 919 fuel rods assembled in a hexagonal array with a pitch of 5.1 cm. The core height is 201 cm. The PARCS model for the BFS core was made with 60° symmetry, 8 planes, and the first coarse group representing Groups 1 through 4 of the 9 groups. The reference solution for this problem was produced through the extrapolation of DIF3D 9-group solutions (Kim, 1999).

The accuracy of the PARCS solutions for the two problems was evaluated in terms of the error in the eigenvalue and the regional group flux or the reaction rate. Tables 1 and 2 list the PARCS solution errors. The maximum flux error of 2% occurring at the control rod region for the lowest energy group of the SNR problem and the eigenvalue error of 25 pcm of the BFS problem prove the excellent accuracy of the multigroup TPEN kernel.

Table 1. Regional Group Flux and Eigenvalue Errors of PARCS for the SNR Problem

Region	Error, %			
	Gr. 1	Gr. 2	Gr. 3	Gr. 4
Inner Core	0.05	0.08	0.09	-0.03
Outer Core	-0.16	-0.07	-0.01	-0.19
Radial Blanket	0.03	-0.26	-0.48	-0.69
Axial Blanket	0.22	-0.11	-0.42	-0.65
Control Rod	0.02	0.16	0.77	2.04
Follower	0.01	0.03	-0.09	0.02
Eigenvalue (Error)	1.00994 (5 pcm)			

Table 2. Reaction Rate and Largest Group Flux Errors of PARCS for the BFS75 Problem

Region	Fission Source Error, %	Max. Error in Group Flux, %
Low Enrichment Zone	-0.02	-0.03
High Enrichment Zone	0.03	0.08
Radial Blanket 1	0.11	0.14
Radial Blanket 2	-0.38	-0.53
Axial Blanket 1	-0.55	-0.62
Axial Blanket 2	-0.37	-0.73
Eigenvalue (Error)	0.99899 (25 pcm)	

In order to examine the computing efficiency of the two-group CMFD formulation to solve multigroup problems, a multigroup CMFD formulation was tried as well. Table 3 compares the two-group vs. multigroup CMFD results. First of all, it should be noted that the number of nodal updates does not reduce much with the multigroup CMFD. This implies that the two-group CMFD formulation has a sufficiently good acceleration capability when used in conjunction with the multigroup TPEN. The number of nodal updates and outer iterations are about 10 and 25, respectively, and they represent a good convergence behavior. In case of the 9-group problem, the saving in the CMFD computing time (on a 733 MHz PC) of the two-group approach is quite significant.

Table 3. Comparison of Iteration Characteristics and Computing Times

		SNR 4G (1/12)		BFS75 9G (1/6)	
		2G CMFD	Multi-G CMFD	2G CMFD	Multi-G CMFD
Number of Nodal Updates		11	10	9	9
Number of Outer Iterations		24	22	22	22
Computing Time, sec	TPEN	0.20	0.18	3.44	3.45
	CMFD	0.05	0.10	0.33	3.21
	Total	0.26	0.29	3.87	6.77

The above results for the two eigenvalue benchmark problems demonstrate that the two-group CMFD formulation with the multigroup TPEN kernel is computationally efficient while delivering highly accurate multigroup solutions. The computational efficiency and the excellent accuracy are other benefits attained over the ease of the implementation of a multigroup feature into an existing two-group code. In the following section, the newly developed multigroup analysis tool is exploited in order to explore the benefits of multigroup calculations.

5. INVESTIGATION OF MULTIGROUP EFFECTS

In order to investigate the group condensation effects in eigenvalue and transient calculations, four sets of group constants were generated with different group structures, 12, 7, 4, and 2 groups, for a model core. Since the error in the homogenized and condensed group constants would diminish with more groups, the 12-group solution can be regarded as the reference. The group constants were generated in a consistent way using the HELIOS code (Stammler, 1994).

5.1 Model Core and Group Constant Generation

The model core is a conceptual core of a medium-sized integral pressurized water reactor (KAERI, 1999) whose thermal output is 330 Mw and no soluble boron is used for reactivity control. The core height is 200 cm and loads 55 hexagonal fuel assemblies. Fig. 3 shows the assembly and core configurations. There are three types of fuel assemblies, all of which use basically 4.95 w/o UO_2 fuels. The assembly pitch is 27.6 cm and 397 rod positions are provided in 11 rings. For the long term reactivity and power distribution control, two types of burnable absorber rods, Gadolinia and B_4C, are used. The control bank arrangement was designed such that the control rods can be inserted into almost all of fuel assemblies (47 out of 55 FAs) in order to reduce the rod worth requirement imposed to each control rod in this boron free reactor.

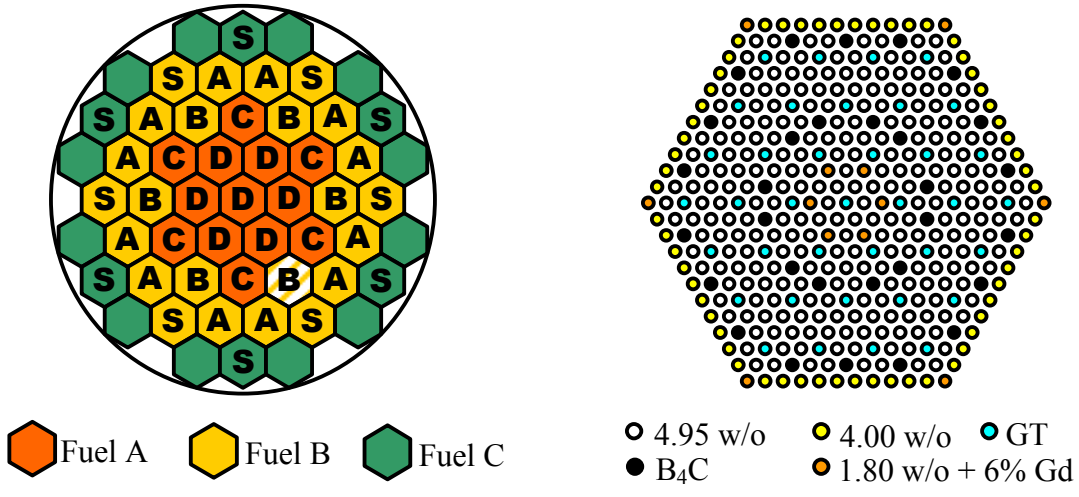

Fig. 3 Fuel Assembly and Core Configurations and Control Bank Arrangement of the Model Core

The group constants were generated with the four group structures shown in Fig. 4. The group boundaries were selected based on the HELIOS's 35 group structure. Note that two groups are allotted in the fission source range in the three multigroup cases. In these two groups, the distinction between the prompt and delayed neutrons can be made.

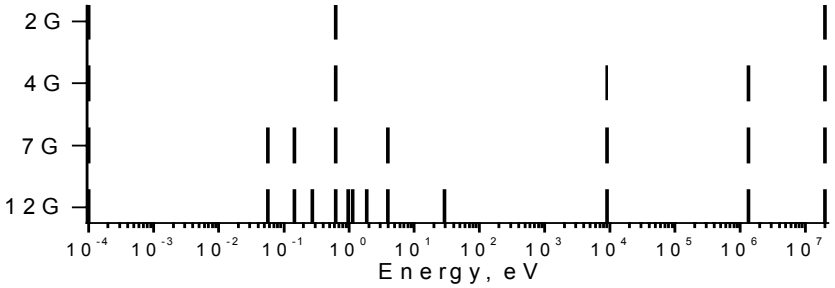

Fig. 4 Energy Group Boundaries of the Four Group Structures Examined

The group constants generated for each composition include assembly discontinuity factors (ADF), fission spectra, and delayed neutron fractions as well as macroscopic reaction cross sections, diffusion constants, and scattering matrices. The delayed neutron fraction generated by HELIOS is the effective delayed neutron fraction (β_{eff}) which accounts for the softer delayed neutron emission spectrum. However, these β_{eff}'s were discarded in the multigroup calculations and instead, the physical values were used with the delayed neutron spectrum explicitly modeled. In addition to the base group constants, their partial derivatives on fuel and moderator temperatures, and the control rod fraction were generated through the variation calculations so that the thermal feedback effects can be incorporated.

5.2 Eigenvalue Calculations

The eigenvalue calculations were performed for the initial states of two control rod ejection cases at a hot-zero-power (HZP) of 0.0001%. In the first case, Bank B is inserted up to 43 cm from the bottom and Bank C is located at 100 cm, while only Bank B is inserted up to 99 cm in the second case. One of the control rods of Bank B, located at the shaded assembly in Fig. 3, is supposed to be ejected in the transient calculation. Eigenvalue calculations for the zero-power ejected state were also performed for each initial condition in order to obtain the static ejected rod worth. The results of the 12-group calculations for the 4 eigenvalue problems are given in Table 4. Taking the 12-group solution as the reference, the errors of the fewer group calculations were evaluated as shown in the table. First of all, it should be noticed that the error of the few group calculation is remarkably small in that the eigenvalue error of the two-group calculations are about 100 pcm and the relative power density (RPD) error is about 1%. There are, however, larger differences noted in the ejected rod worth (ERW). The two-group ERW is under-predicted by 2.7% for the first case, which is rodded more heavily, whereas it is over-predicted by 1.5% for the second case, which is rodded with only Bank B. The consequence of the error in the ERW appears in the transient core power behaviors shown

in Fig. 5. The static ERW of the two cases in dollars are 1.13 and 1.04$, respectively (β=0.00746).

Table 4. Eigenvalue Calculations Results for the Initial and Rod-out States

		Initial State			Rod-out State			ERW (pcm) & Err (%)
		k_{eff} & Error (pcm)	Max. RPD & Err (%)	Min. RPD & Err (%)	k_{eff} & Error (pcm)	Max. RPD & Err (%)	Min. RPD & Err (%)	
Banks B & C Inserted	12G	0.96885	1.1888	0.6702	0.97682	2.7698	0.3447	842.3
	7G	10.4	-0.04	0.05	7.1	-0.04	0.08	-0.39
	4G	70.9	-0.59	1.12	50.5	-0.44	1.16	-1.58
	2G	104.5	-0.75	1.32	82.1	-0.55	1.52	-2.66
Bank B Inserted	12G	1.00259	1.3034	0.5721	1.01047	2.7558	0.3052	777.6
	7G	-0.1	-0.05	0.04	-1.2	0.01	0.01	-0.14
	4G	30.7	-0.64	1.01	31.0	-0.01	0.50	-0.11
	2G	39.1	-0.39	1.16	50.5	0.35	0.09	1.47

5.3 Transient Calculations for Control Rod Ejection

The transient core power behaviors obtained with multigroup formulations agree with each other fairly well as shown in Fig. 5. The two-group case, however, is quite different from the reference, especially for the first case. The peak of the two-group case comes later with a much lower magnitude. One reason for this later peak is the smaller rod worth. Another reason is that the softer delayed neutron spectrum cannot be distinguished from the prompt neutron spectrum in the two-group calculation. The consequence is that the leakage of the delayed neutrons is exaggerated and thus the reactivity is lowered. A corrective measure for this two-group specific problem is to reduce the *physical* beta by a certain fraction to yield an *effective* beta. A 3% reduction of beta yields the dotted curves in the graph. The artificial adjustment factor seems to work quite well for the first case. However, in the second case in which the two-group ERW is over-predicted, the adjustment factor causes a too high peak. Since the two-group ERW can be either over- or under-predicted, a fixed delayed neutron adjustment factor should be used with caution. Although the impact of group condensation appears negligible in the steady-state cases, the consequence of a small error can be significant in fast super-prompt critical transients as demonstrated by Fig. 5. Therefore, it is recommended to perform multigroup calculations if the transient analysis involves critical results.

The computational performance of the two-group CMFD based multigroup calculations are shown in Table 5 in terms of the number of CMFD and TPEN solutions and the total computing time for the 1-second transient performed with 100 time steps. As shown in the table, the number of solutions does not vary much with different group structures. The fact that the number of TPEN calculation is much less than 100 is due to that the TPEN calculations are skipped in some time steps because of the conditional nodal update logic implemented in PARCS. This feature can save the computing time of

the multigroup calculation significantly. It is noted that the total computing time increases slightly faster than linearly with the number of groups.

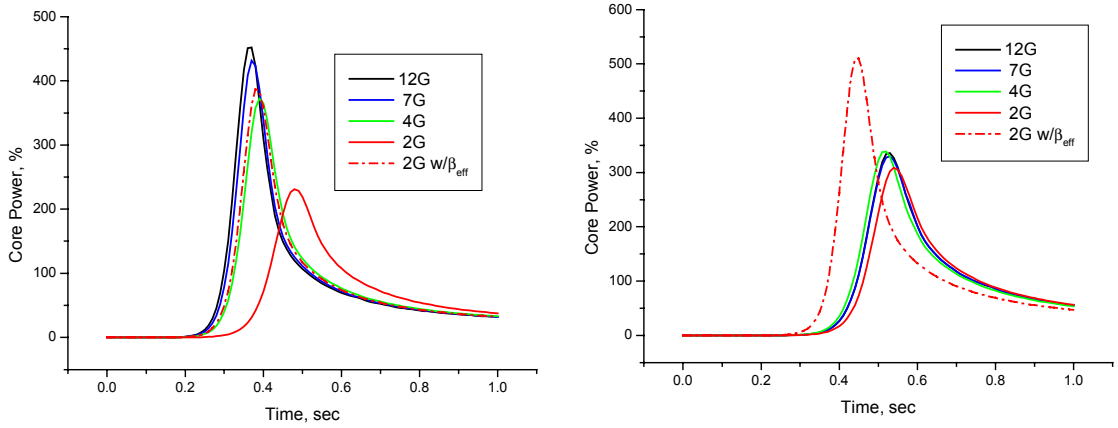

Banks B & C Inserted Initially Bank B Only Inserted Initially

Fig. 5 Rod Ejection Calculation Results Obtained with Various Group Structures

Table 5. Number of Iterations and Computing Time for the 1 sec Rod Ejection Transient (CPU Time Measured in Seconds on a 733 MHz Pentium III PC)

	12G			7G			4G			2G		
	N_{CMFD}	N_{TPEN}	CPU	N_{CMFD}	N_{TPEN}	CPU	N_{CMFD}	N_{TPEN}	CPU	N_{CMFD}	N_{TPEN}	CPU
Case 1	330	66	120.7	339	68	55.2	337	66	35.0	337	59	13.9
Case 2	341	60	115.6	346	64	53.6	353	61	33.1	350	62	14.3

6. CONCLUSIONS

A two-group CMFD formulation capable of multigroup calculations has been established through a dynamic condensation scheme. The TPEN multigroup one-node nodal kernel was developed such that it can yield uniquely a multigroup spectrum as well as multigroup interface currents for a hex-octahedron node. The accuracy of the proposed multigroup solver is superior as demonstrated by the eigenvalue benchmark solutions. The computational efficiency gained by the two-group CMFD formulation enables rapid multigroup transient calculations. The multigroup calculations for a model core show that the current two-group solution approach involves only trivial error in eigenvalue calculations, but in transient calculations, the error in the predicted core power behaviors can be significant due to small errors in the ejected rod worth as well as the inability of distinguishing the delayed and prompt neutron spectra. The fast multigroup calculation method proposed here can be used for more extensive multigroup transient calculations and for more accurate analyses of the advanced fuel cycle designs involving MOX or thorium.

ACKNOWLEDGMENTS

This work was performed under the long-term nuclear research and development program sponsored by the Ministry of Science and Technology of Korea.

REFERENCES

ANL, 1985. Argonne National Laboratory Code Center Benchmark Problem Book, ANL-7416, Suppl. 3, p 861, Argonne National Laboratory, Dec. 1985.

Cho, B. O, *et. al.*, 1999. MASTER-2.0: Multi-purpose Analyzer for Static and Transient Effects of Reactors, KAERI/TR-1211/99, Korea Atomic Energy Research Institute.

Cho, J. Y, Joo, H. G., Cho, B. O., and Zee, S. Q., 2001. Hexagonal CMFD Formulation Employing a Triangle-Based Polynomial Expansion Nodal Kernel, *Proc. M&C 2001*, Salt Lake City, Utah, Sept. 2001, to appear.

KAERI, 1999. Development of Core Design and Analyses Technology for Integral Reactor, KAERI/RR-1885/98, Korea Atomic Energy Research Institute, March 1999.

Kim, T. K, *et. al.*, 1999. Development of a Multi-Group, Multi-Dimensional Simplified P2 Transport Code, SOLTRAN, in Hexagonal Geometry, KAERI/TR-1449/1999, Korea Atomic Energy Research Institute.

Joo, H. G., Barber, D., Jiang., G., and Downar, T. 1998. PARCS: A Multi-Dimensional Two-Group Reactor Kinetics Code Based on Nonlinear Analytic Nodal Method, PU/NE-98-26, Purdue University, Sept. 1998.

Stammler, R., 1994. HELIOS Program Description, Scanpower.

Sutton, T. and Aviles, B. N., 1996. Diffusion Theory Methods for Spatial Kinetics Calculations, *Prog. Nucl. Ener.*, **30**, 119-182.